Assembly of One to Four As_4 Analogues, $(Ge_2As_2)^{2-}$ or $(Ge_3As)^{3-}$, in the Coordination Sphere of $[PhM]^+$, $[MesM]^+$, or M^{2+} (M = Zn, Cd, Hg)

*Shangxin Wei, Benjamin Peerless, Lukas Guggolz, Stefan Mitzinger, and Stefanie Dehnen**

Dedicated to Professor Klaus Jurkschat on the occasion of his 70th birthday.

Abstract: *Pseudo*-tetrahedral units of p-block atoms proved to be excellent building blocks for novel molecular architectures and for introducing new elemental combinations which are not otherwise accessible. In this work, we present a series of clusters obtained by reactions of binary Ge/As anions with $[MPh_2]$ (M = Zn, Cd, Hg; Ph = phenyl). The study is grounded on the fact that the binary reactant gained by extracting the solid 'K_2GeAs' with ethane-1,2-diamine (en) co-exists as $(Ge_2As_2)^{2-}$ and $(Ge_3As)^{3-}$ in solution. This allows for a larger variety of products by 'selecting' the most suitable species for the final ternary complex to crystallize. The reactions afforded the unprecedented first step of the corresponding interaction, thus attachment of $(MPh)^+$ to a *pseudo*-tetrahedral unit in $[PhZn(Ge_3As)]^{2-}$ (**1**) and $[PhHg(Ge_3As)]^{2-}$ (**2**), and complex anions with two, three, or four units, $[(Ge_3As)Zn(Ge_2As_2)]^{3-}$ (**3**), $[Cd_3(Ge_3As)_3]^{3-}$ (**4**), and $[Zn_3(Ge_3As)_4]^{6-}$ (**5**). Quantum chemistry confirmed the compositions and the positions of the Ge or As atoms, beside explaining structural peculiarities. The subtle impact of different $[MR_2]$ reactants was additionally studied by corresponding reactions using $[ZnMes_2]$ (Mes = mesityl), which showed success in selectively crystallizing $[MesZn(Ge_3As)]^{2-}$ (**6**). Based on our findings, we derive a suggestion of the underlying reaction cascade.

Introduction

Tetrahedral molecules of the type E_4^{q-} (E = p-block element; q = 0–4) are known for several elements of the p-block. White phosphorus, P_4, being the archetypal example, plays a vital role in many industrial processes as a precursor for the synthesis of organophosphorus compounds.[1] In a more academic sense, the activation of P_4 with transition metal and main group complexes has yielded a diverse number of phosphorus species ranging from metal-phosphorus triple bond, metal-P_4 complexes and to poly-phosphorus species with tens of phosphorus atoms.[2] By the *pseudo*-element concept, exchanging the phosphorus atoms with other group 15 atoms and with (negatively charged) group 13 or group 14 atoms provided the foundation for the exploration of other homoatomic tetrahedral Tt_4^{4-} molecules (Tt = Si, Ge, Sn, Pb), As_4, and further to heteroatomic species P_3As, $(TrBi_3)^{2-}$ (Tr = Ga, In, Tl), and $(Tt_2Pn_2)^{2-}$ (Tt/Pn = Ge/P, Ge/As, Ge/Sb, Sn/Sb, Sn/Bi, Pb/Sb, Pb/Bi).[3] The use of these main group tetrahedra as ligands to transition metal atoms has a long tradition for P_4, and more recently became obvious for some of the others, too. The use of d^{10} metal compounds has shown great promise in this regard, as these redox inert species ensure that the respective tetrahedron remains intact. Starting from a solid-state approach, Cs_6Ge_8Zn, which contains two types of $(ZnGe_8)^{6-}$ anions, was thus synthesized through the fusion of Cs/Zn/Ge elements at 900 °C.[4] Similarly, the oligomeric $[Pb_4CdPb_4CdPb_4CdPb_4]^{10-}$ and infinite chain-like extensions of $_\infty^1[Au(\eta^2{:}\eta^2\text{-}Tt_4)]^{3-}$ (Tt = Sn, Pb) and $_\infty^1[Au(\eta^2{:}\eta^2\text{-}TlSn_3)]^{4-}$ have also been obtained by investigating solids with a composition of K_6Pb_8Cd, Cs_3AuTt_4 and $K_4AuTlSn_3$, respectively.[3c,5] Extension into solution reactions saw a different approach, where the source of the d^{10} metal atoms was in the form of an organometallic complex. Using liquid ammonia as solvent in the presence of sequestering agents such as 1,4,7,10,13,16-hexaoxacyclooctadecane (18-crown-6) and 4,7,13,16,21,24-Hexaoxa-1,10-diazabicyclo-[8.8.8]hexacosane (crypt-222),[6] the first examples isolated were a series of $[(MesCu)_2(\eta^3,\eta^3\text{-}Tt_4)]^{4-}$ ($Tt_4 = Si_4$, Ge_4, $Si_{3.3}Ge_{0.7}$; Mes = mesityl) complexes with four-atom units bridging two MesCu fragments.[7] Examples without organic substituents bound to the metal atom demonstrated the ability of anionic tetrahedral molecules to function as terminal ligands to metal centers, affording complexes of the general formula $[(Tt_4)_2M]^{q-}$ such as $[Zn(\eta^3\text{-}(Ge)_4)_2]^{6-}$,[4] $[(\eta^3\text{-}Ge_4)Zn(\eta^2\text{-}Ge_4)]^{6-}$,[7c] $[Zn(\eta^2\text{-}(Si/Ge)_4)_2]^{6-}$,[8] $[Au(\eta^2\text{-}Sn_4)_2]^{7-}$,[9] and $[(\eta^2\text{-}Sn_4)Zn(\eta^3\text{-}Sn_4)]^{6-}$,[10] which were obtained as ammoniates of their alkali metal salts from extraction

[*] S. Wei, Dr. B. Peerless, Dr. L. Guggolz, Dr. S. Mitzinger, Prof. Dr. S. Dehnen
Karlsruhe Institute of Technology (KIT), Institute of Nanotechnology
P.O. Box 3640, 76021 Karlsruhe (Germany)
E-mail: stefanie.dehnen@kit.edu

solutions of Zintl phases in liquid ammonia[8,9,10] or as neat solids by solid state reactions.[4,7c] A larger supertetrahedral cluster, $[M_6Ge_{16}]^{4-}$ built up from Ge_4^{4-} clusters and either Zn or Cd atoms was also achieved by reaction of such solids with organometallic complexes.[11]

Analogous heteronuclear tetrahedral clusters of Tt and Pn elements, i.e., $(Tt_2Pn_2)^{2-}$, have also been shown to coordinate to d^{10} metal atoms, namely in the example of $[Au\{\eta^2\text{-}(Sn_2Sb_2)\}_2]^{3-}$.[12] For $(Ge_2P_2)^{2-}$ and $(Ge_2As_2)^{2-}$, there is a distinct change in the chemistry of the reaction between these salts and coinage and other d^{10} metal complexes. The pinwheel-like shaped $[Cd_3(Ge_3P)_3]^{3-}$ and the supertetrahedral $[Au_6(Ge_3As)(Ge_2As_2)_3]^{3-}$ clusters both exhibit an exchange of the atomic composition in the parent *pseudo*-tetrahedron on cluster formation from a Ge/Pn ratio of 2:2 to 3:1.[3g,13] This exchange process appears to be a property inherent to the elements the tetrahedron is comprised of. Two aspects dictate the reactivity pathway of heteronuclear clusters that are both related to the atomic size of the elements involved: the difference in the atomic radii of the elements in the cluster and the general size of the elements themselves.[3o] Tetrahedral clusters containing heavy atoms, such as $(Pb_2Bi_2)^{2-}$ and $(TlBi_3)^{2-}$, undergo a series of fragmentation and reorganization steps, or release of elemental metals, which ultimately yield larger clusters with the original tetrahedron being usually, although not always, lost in the process.[14a] In contrast, those tetrahedral clusters with lighter elements (Ge, P, As) predominantly maintain their tetrahedron structure, as shown with the examples above. The examples of $(Sn_2Sb_2)^{2-}$ and $(Pb_2Bi_2)^{2-}$ in contrast, represent perfectly matched elements for size, but are (relatively) heavy. Therefore, there are situations where the tetrahedron is intact on cluster formation, like in $[Au\{\eta^2\text{-}(Tt_2Pn_2)\}_2]^{3-}$,[12,14b] and also where fragmentation processes occur, such as in $\{[CuSn_5Sb_3]^{2-}\}_2$.[14c] The balance of the reaction pathway not only lies with the cluster elements, but also with the organometallic reagent used. Understanding this balance is one of the keystones for the prediction of cluster formation pathways and remains as a significant challenge.

Over the past several years, we have used both salts of binary *pseudo*-tetrahedral p-block anions and also ternary solids as in situ sources for said anions and discerned their properties and follow-up chemistry. As one of our endeavors is to elucidate cluster growth steps, we have chosen to react the ternary solid 'K_2GeAs', as a source for stable 4-atom anions, with redox-inert group 12 organometallics hoping to gain access to a diverse family of clusters with intact *pseudo*-tetrahedral units of main group atoms. Herein, we report the success of this approach with the isolation of new clusters of group 12 metals and Ge/As tetrahedra.

Results and Discussion

Our work was inspired by the seminal work using $[MPh_2]$ complexes along with Tt_9^{4-} Zintl anions (Tt = Ge, Sn).[15] Reactions between 'K_2GeAs' and $[MPh_2]$ (M = Zn, Cd, Hg) and $[ZnMes_2]$ in an ethane-1,2-diamine (en) suspension in the presence of the sequestering agent crypt-222 yielded a series of single-crystalline $[K(crypt\text{-}222)]^+$ salts of new ternary Zintl anions, $[PhZn(Ge_3As)]^{2-}$ (**1**), $[PhHg(Ge_3As)]^{2-}$ (**2**), $[(Ge_3As)Zn(Ge_2As_2)]^{3-}$ (**3**), $[Cd_3(Ge_3As)_3]^{3-}$ (**4**), $[Zn_3(Ge_3As)_4]^{6-}$ (**5**), and $[MesZn(Ge_3As)]^{2-}$ (**6**), see Scheme 1.[16]

Typically, the extraction and subsequent crystallization of ternary K/Tt/Pn solids with en and crypt-222 leads to the exclusive formation of salts of the composition $[K(crypt\text{-}222)]_2(Tt_2Pn_2)$. This applies to '$K_2GeAs$', too. However, from the compounds obtained here, it is obvious that other species than an anion with a 2:2 composition of the p-block atoms seem to co-exist in solution. We have previously shown that for a potential equilibrium between two equivalents of $(Ge_2As_2)^{2-}$ and one equivalent each of $(Ge_3As)^{3-}$ and $(GeAs_3)^-$, the formation of the latter is significantly energetically favored.[13] To confirm this to happen during the extraction process, in situ electrospray ionization mass spectrometry (ESI-MS) measurements were recorded. The spectrum after five minutes of stirring (see Figure S26) indeed shows signals of $(Ge_3As)^-$ at *m/z* 292.7, $(Ge_3AsH_2)^-$ at *m/z* 294.7, $(Ge_2As_2H)^-$ at *m/z* 296.7, and $(GeAs_3)^-$ at *m/z* 298.7 (note that Zintl anions can survive ESI-MS conditions even under oxidation). This clearly demonstrates the coexistence of these different binary species upon extraction of 'K_2GeAs'. Apparently, group 12 organometallics seem to show a tendency to react with both the $(Ge_2As_2)^{2-}$ and the $(Ge_3As)^{3-}$ anion owing to the relatively high Lewis acidity of both $(MPh)^+$ and M^{2+}. The order of interaction with one or the other *pseudo*-tetrahedral species allows for some selectivity in the product spectrum: if $(Ge_2As_2)^{2-}$ is coordinated first, the only product to form will be **3**, while initial coordination of $(Ge_3As)^{3-}$ can lead to any of the anions **1**–**5** (see Scheme 1). We ascribe the order of interaction to kinetic reasons, which includes relative concentrations of the anions.

Considering the reaction between 'K_2GeAs' and $[ZnPh_2]$ first, addition of en to an optimized 2:1:3 (molar) mixture of 'K_2GeAs', $[ZnPh_2]$ and crypt-222 afforded an orange suspension. ESI-MS of the filtered reaction mixture showed several signals of which a number of Zn/Ge/As containing

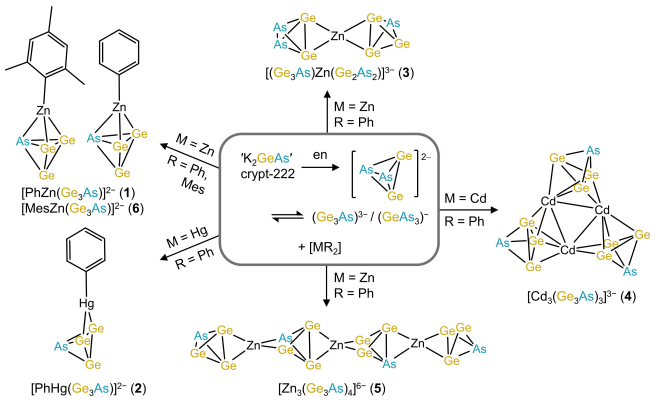

Scheme 1. Summary of the reactions of an extraction solution of the solid 'K_2GeAs' in 1, 2-diaminoethane (en) with $[MPh_2]$ (M = Zn, Cd, Hg) and $[ZnMes_2]$ yielding the complex anions **1**–**6**.

species could be assigned (see Figure S76–S78), the most relevant of which are $[K_2Zn_3Ge_9As_3]^-$, $[K_2(crypt\text{-}222)Zn_3Ge_9As_3]^-$ and $[K_2(crypt\text{-}222)_2Zn_3Ge_9As_3]^-$ (note that the monoanionic nature of the species typically detected in ESI-MS studies of Zintl anions does not refer to their original charge, but are a result of a rapid in situ oxidation during the measurement).

Filtration and layering of the solution with toluene and storage at 5 °C for two days led to the formation of a large quantity of orange needle-shaped crystals. A combination of single crystal X-ray diffraction and micro X-ray fluorescence spectroscopy (μ-XFS) revealed $[K(crypt\text{-}222)]_2[PhZn(Ge_3As)]_{0.9}\cdot(Ge_2As_2)_{0.1}\cdot 0.9tol$ ($[K(crypt\text{-}222)]_2$-(**1**)$_{0.9}\cdot(Ge_2As_2)_{0.1}\cdot 0.9tol$) as their composition. If the solution was stored for longer, the needle-shaped crystals start to disappear after a few days, while two new crystalline products grow over 21 days. These were identified as $[K(crypt\text{-}222)]_3[(Ge_3As)Zn(Ge_2As_2)]$ ($[K(crypt\text{-}222)]_2$(**3**)) and $[K(crypt\text{-}222)]_9[Zn_3(Ge_3As)_4]_{1.5}\cdot en$ (with two different conformers of the anion, **5a** and **5b**, in $[K(crypt\text{-}222)]_9$(**5a**)-(**5b**)$_{0.5}\cdot en$). Observation of these two compounds together with **1** provides insight both into the coexistence of $(Ge_2As_2)^{2-}$ and $(Ge_3As)^{3-}$, and the stepwise growth (and crystallization) of the ternary assemblies using these species: exchange of one of the phenyl groups on the Zn atom with $(Ge_3As)^{3-}$ affords anion **1** as the first step; exchange of the second phenyl group with $(Ge_2As_2)^{2-}$ yields anion **3**; if $(Ge_3As)^{3-}$ were used in this step instead (with a hypothetical anion '$[Zn(Ge_3As)]^{3-}$' (**3'**) being produced), a continuation of the process with two further equivalents of both $[ZnPh_2]$ and $(Ge_3As)^{3-}$ allows anion **5** to form and crystallize. The latter demonstrates the degree of freedom that is added to the reaction space by the two coexisting binary building units. We note in addition that other reactant stoichiometries than the ones used here did not alter the product spectrum.

On changing from $[ZnPh_2]$ to $[HgPh_2]$, under slight variation of the reactant (molar) ratio to 3:1:3, the reaction appears to stop at $[K(crypt\text{-}222)]_2[PhHg(Ge_3As)]\cdot tol$ ($[K(crypt\text{-}222)]_2$(**2**)$\cdot$tol) and no further products were observed. Interestingly, despite an analogous elemental composition between **1** and **2**, a difference in the coordination mode of the $(Ge_3As)^{3-}$ *pseudo*-tetrahedron is observed, η^3-Ge_2As and η^2-Ge_2 respectively (discussed further below). With respect to $[CdPh_2]$, only the pinwheel-like structure $[K(crypt\text{-}222)]_3[Cd_3(Ge_3As)_3]\cdot tol$ ($[K(crypt\text{-}222)]_3$(**4**)$\cdot$tol), analogous to the previously reported $[K(crypt\text{-}222)]_3[Cd_3(Ge_3P)_3]$,[3g] was obtained upon reacting a 2:1:3 (molar) mixture of 'K_2GeAs', $[CdPh_2]$ and crypt-222. Notably, although a corresponding Zn compound was not isolated, a species with the elemental composition $(Zn_3Ge_9As_3)^-$ was observed in the ESI mass spectrum (see above), which suggests that the same pinwheel-like structure can also form with the lightest group 12 metal. In fact, a poor-quality diffraction pattern was obtained of some crystals which appeared to show this anion.

The low quantities of $[K(crypt\text{-}222)]_2$(**2**)$\cdot$tol and $[K(crypt\text{-}222)]_3$(**4**)$\cdot$tol obtained in these experiments gives rise to the question as to the fate of the rest of the reactants. In the mother liquor upon crystallization of both compounds, no meaningful signals were identifiable by ESI mass spectrometry owing to very low concentrations upon doubling the volume of solvent by layering. Inspection of the reaction solution by ESI-MS of the $[HgPh_2]$ experiment, showed only anion **2**. Interestingly, on dissolution of $[K(crypt\text{-}222)]_2$(**2**)$\cdot$tol in DMF, the ESI-MS measurement did not show a signal of **2**. Instead, a new anion with composition of $(K(crypt\text{-}222)HgGe_5As_3H)^-$, hence an analogue of **3**, was observed (with a very low intensity though, and aggregated with one counterion and one proton in the gas phase). In the case of $[CdPh_2]$, the in situ ESI mass spectrum indicates the formation of transient species in very low concentrations containing Cd, Ge, and As (according to the isotope patterns); however, none of the compositions accords with any isolable anionic cluster, thus suggesting a relatively high reactivity of the (smaller) Cd-based species. Similarly to the Hg example, the ESI-MS measurement of redissolved crystals of $[K(crypt\text{-}222)]_3$(**4**)$\cdot$tol in DMF showed a signal for $(CdGe_5As_3C_7H_{10})^-$, indicating the formation of a Cd analogue of **3** (see also below). This can be understood as a reversal of the formation of **4** from **3**, thus indicating the clusters' relationship. Although these spectra were of a rather low intensity, the findings shed light onto similar cluster formation processes to take place with Zn, Cd, and Hg complexes, yet with different reaction rates and yield.

The range of products obtained from this series of organometallic complexes hints to the subtle effect the nature of the transition metal has on the reaction path. One possible explanation is the differing relative charge located at the respective metal atom in the starting material and products (further discussed later with respect to differing coordination modes observed in **1** and **2**).

Another parameter may be the role of the organic substituent. To provide further insight into this possibility, we exchanged $[ZnPh_2]$ with $[Zn(Mes)_2]$ and $[Zn(C_6F_5)_2]$ in an effort to reduce or increase the tendency to release the ligand, respectively, of the Zn-based starting material. We also considered $ZnCl_2$ as an alternative although we have had very little success using binary metal halides in the past. On reaction between 'K_2GeAs' and $[Zn(Mes)_2]$, crystals were obtained following the procedure described with $[ZnPh_2]$ that were identified as the analogous salt $[K(crypt\text{-}222)]_2[MesZn(Ge_3As)]$ ($[K(crypt\text{-}222)]_2$(**6**)). No further products were obtained, and the only assignable signals in an in situ ESI-MS measurement of the reaction solution showed variations of only one *pseudo*-tetrahedron per Zn atom (see Section 4 of the Supporting Information). Signals at higher m/z ratios are present, however could not be assigned and did not fit to any of the known analogous further substituted compounds. Neither $ZnCl_2$ or $[Zn(C_6F_5)_2]$ afforded any conclusive evidence, and decomposition was all that was observed. To corroborate the experimental studies, comprehensive quantum chemical calculations using density functional theory (DFT) methods[17] were performed to investigate the different $[RM(Ge_3As)]^{2-}$ (M = Zn, Cd, Hg; R = Ph, Mes, C_6F_5) combinations as well as their respective reaction energies

towards exchange of the organic groups by Zintl anions. It could be shown that all of these anions should in principle be stable and synthesizable (Figures S93 and S94, and Scheme S1).

It is worth noting that, neither the ratio nor the exact atomic position of the Ge/As atoms in the compounds reported herein can be distinguished by X-ray diffraction alone. Therefore, within the structure models of all compounds reported, the positions of the Ge and As atoms have been statistically refined over all atom sites in the *pseudo*-tetrahedra. The atomic compositions were rationalized by means of the *pseudo*-element concept in accordance with the total charges of the product clusters and confirmed by μ-XFS studies, the combination of which also ruled out protonation of any of the clusters in the crystalline products. The most probable site occupancies were elucidated using DFT calculations, the results of which are illustrated in the structure Figures by a predominance of the respective atom color (yellow = Ge, blue = As) in the two-colored thermal ellipsoids.

The single crystal structure analyses of $[K(crypt\text{-}222)]_2(\mathbf{1})_{0.9}\cdot(Ge_2As_2)_{0.1}\cdot 0.9tol$ and $[K(crypt\text{-}222)]_2(\mathbf{2})\cdot tol$ show both anions with a general formula of $[PhM(Ge_{4-x}As_x)]^{2-}$ (for M = Zn in combination with a 10 % co-crystallization of the $(Ge_2As_2)^{2-}$ anion). However, the coordination mode of the *pseudo*-tetrahedron differs between the Zn and Hg compounds (Figure 1, top and center). The presence of two $[K(crypt\text{-}222)]^+$ molecules observed in the structures indicate an anion possessing an overall charge of 2− , and, consequently, the *pseudo*-tetrahedron therefore has a 3− charge and a composition of Ge:As of 3:1. In both molecules, the coordination of the tetrahedron was shown to have a preference for the atoms of a Ge– Ge bond by DFT calculations (discussed in more detail below) with different emphasis. The $(PhZn)^+$ unit in **1** is coordinated by the $(Ge_3As)^{3-}$ tetrahedron in a η^3-Ge_2As fashion, similar to complexes containing d^{10} transition metal fragments and Ge_4^{4-}, such as $[(EtZn)_2(\eta^3{:}\eta^3\text{-}Ge_4)]^{2-}$ and $[(MesCu)_2(\eta^3{:}\eta^3\text{-}Ge_4)]^{4-}$.[7c,17] However, the Zn atom does not sit exactly above the center of the triangular face, but rather offset towards the Ge– Ge bond. In **2**, the coordination mode is only η^2-Ge_2 with no significant As contribution at all. The difference in the coordination mode can be seen clearly in different dihedral angles between the Ge_3 faces and the Ge_2M planes of **1** compared to **2** (148.3° vs. – 164.2°).

DFT calculations served to determine the atom assignment (Figure 2). Capping of the Ge_2As face (Figure 2a) instead of the Ge_3 face (Figure 2b) in **1** seems counterintuitive at first. However, inspection of the canonical molecular orbitals (MOs) of the parent $(Ge_3As)^{3-}$ *pseudo*-tetrahedron (see Figure S95)[13] showed the doubly-degenerate highest occupied molecular orbital (HOMO) to mainly represent the Ge– Ge bond with a minor contribution of the As atom, while HOMO– 1 is found in the center of the trigonal Ge_3 face. Thus, the experimentally found conformer of **1** is energetically favored by 11 kJ·mol^{-1} over the conformer in which the $(PhZn)^+$ fragment caps the Ge_3 face.

A complete neglect of the Zn···As interaction would be disadvantaged by 14 kJ·mol^{-1} (Figure 2c). However, local-

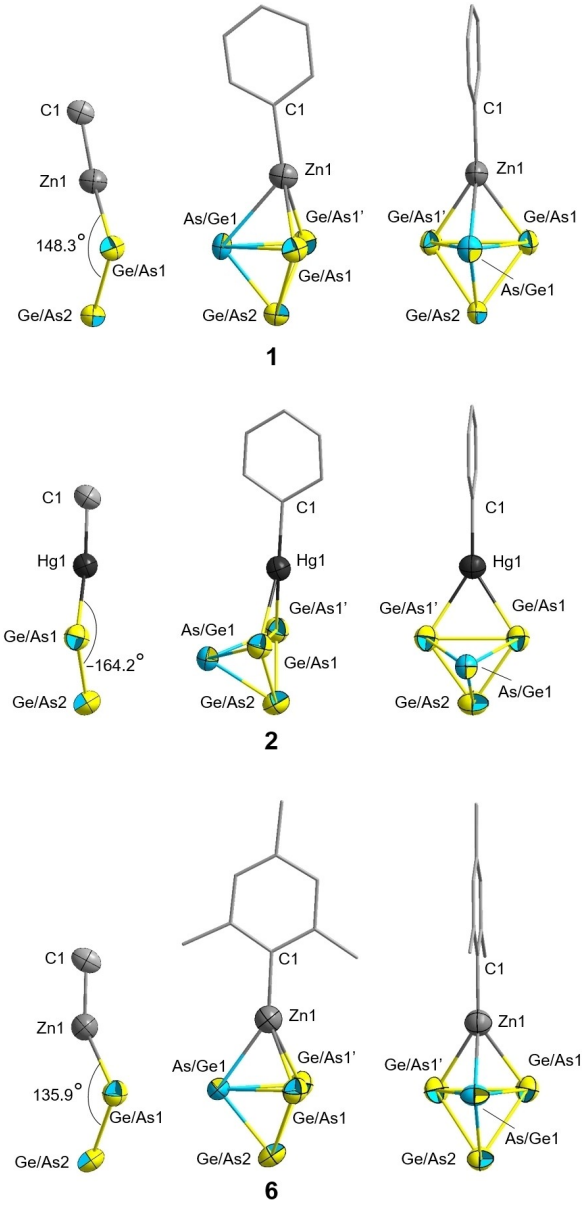

Figure 1. Side views (left and center) and front view (right) of the molecular structures of the anions $[PhZn(Ge_3As)]^{2-}$ (**1**) in compound $[K(crypt\text{-}222)]_2(\mathbf{1})_{0.9}\cdot(Ge_2As_2)_{0.1}\cdot 0.9tol$, $[PhHg(Ge_3As)]^{2-}$ (**2**) in compound $[K(crypt\text{-}222)]_2(\mathbf{2})\cdot tol$, and $[MesZn(Ge_3As)]^{2-}$ (**6**) in compound $[K(crypt\text{-}222)]_2(\mathbf{6})$] with thermal ellipsoids drawn at 50 % probability. Since Ge and As atoms cannot be distinguished, the corresponding atom types are drawn in two-colored fashion (yellow-blue), with the more probable atom according to quantum chemical calculations being indicated by the dominant color (see text). Selected distances [Å] and angles [°] in **1**: Zn C 2.037(11), Zn Ge/As1 2.4525(17), Zn As/Ge1 2.657(2), Ge/As1 As/Ge1 2.5983(15), Ge/As1 Ge/As1′: 2.758(3); C Zn Ge/As 145.42(6), C Zn As/Ge 131.3(3), Ge/As Zn Ge/As 68.41(7), Ge/As Zn As/Ge 60.98(5). Selected distances [Å] and angles [°] in **2**: Hg C 2.123(16), Hg Ge/As1 2.6394(13), Ge/As1 As/Ge1 2.4804(15), Ge/As1 Ge/As1′ 2.830(2); C Hg Ge/As 147.18(7), Ge/As Hg Ge/As 64.84(5), Hg Ge/As1 Ge/As1′ 57.58(3), Hg Ge/As1 As/Ge1 91.62(5), Hg Ge/As1 Ge/As2 111.34(5). Selected distances [Å] and angles [°] in **6**: Zn C 1.970(9), Zn Ge/As1 2.5237(12), Zn As/Ge1 2.4920(15), Ge/As1 As/Ge1 2.6538(10), Ge/As1 Ge/As1′: 2.6377(14); C Zn Ge/As 140.00(17), C Zn As/Ge 147.1(3), Ge/As Zn Ge/As 63.01(4), Ge/As Zn As/Ge 63.89(4).

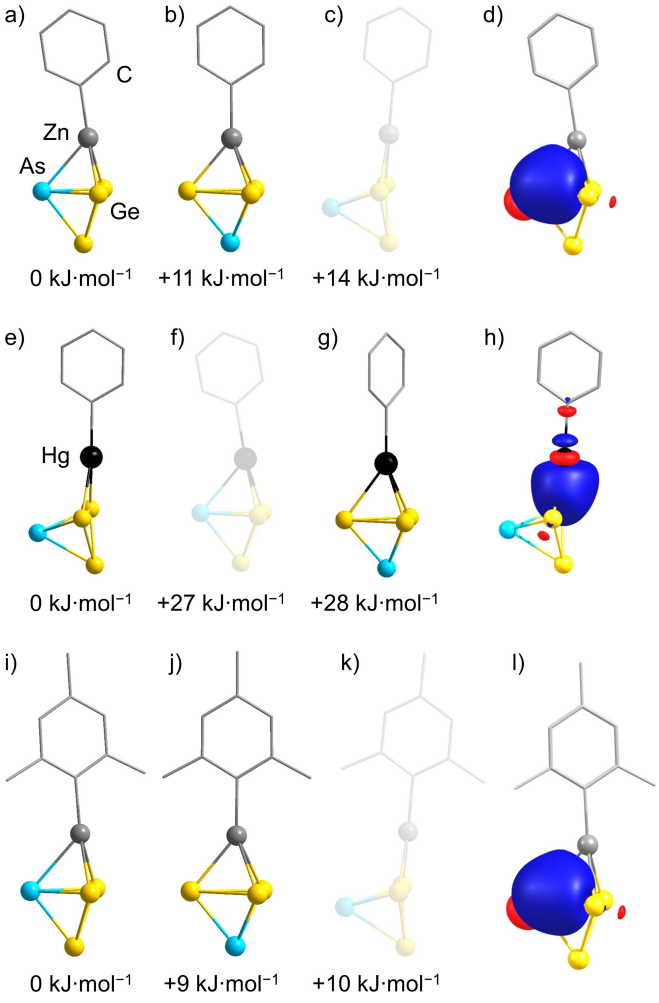

Figure 2. Computationally optimized minimum structures of the possible conformers of **1** (a–c), **2** (e–g), and **6** (i–k), as well as LMOs of (d, l) one of two equivalent weak two-electron-three-center Zn Ge As interactions of the *pseudo*-tetrahedral moiety with the respective $(RZn)^+$ fragment and (h) of the two-electron-three-center interaction of the *pseudo*-tetrahedral moiety with the $(PhHg)^+$ fragment. H atoms are omitted in the images for clarity. Conformers that were computed with constrained dihedral angles for comparison are shown in semi-transparent mode. Contour values are drawn at ±0.05 a.u.

ization of the molecular orbitals to form localized molecular orbitals (LM Os) and population analyses showed that the Zn···As interaction is weaker than the Zn– Ge bonds. This is the reason why the $(PhZn)^+$ fragment additionally is not situated symmetrically above the Ge_2As face (Figure 2d).

In contrast to the Zn atom in **1**, the Hg atom in **2** has a trigonal coordination sphere (Figure 2e). So, the Ge– Ge bond of the *pseudo*-tetrahedral moiety coordinates to it in an η^2-Ge_2 fashion (Figure 2h), while an interaction with the Ge_2As or the Ge_3 faces (Figures 2f, 2 g) would be disadvantaged by 27 or 28 kJ·mol^{-1}, respectively. This can be explained with the calculated Mulliken partial charges of the respective metal atoms in the $(PhM)^+$ fragment (+0.7 for Zn and +0.6 for Hg). The tendency to compensate for the higher positive charge by interacting with the more negatively polarized As atom of the parent $(Ge_3As)^{3-}$ anion (−0.9 vs. −0.7 for the Ge Atom) is thus stronger for the Zn atom. A better compensation of the positive charges is probably also the reason why the $(PhM)^+$ fragments—at least in this case—interact more readily with the $(Ge_3As)^{3-}$ anions, than with the $(Ge_2As_2)^{2-}$ anions, due to the higher overall charge of the former, eventually leading to the formation of **1** and **2**.

Similarly, the anion in $[K(crypt\text{-}222)]_2$(**6**) (Figure 1, bottom) has an analogous structure to **1**. The *pseudo*-tetrahedron is coordinated in an η^3-Ge_2As fashion, however, the Zn atom is more aligned to the center of the Ge_2As triangle and has a more symmetric coordination environment. The bond length range between Zn–Ge/As is narrower in **6** than **1** (2.4920(15), 2.5237(12) Å vs. 2.4525 (17), 2.657(2) Å, respectively), and is equally reflected in the Ge/As–Zn–Ge/As bond angles. This, however, seems to be a steric effect in the crystal structure. The computationally obtained minimum structure of **6** exhibits the same elongation of the Zn–As bond, as found in **1** (Tables S12 and S13). DFT calculations also show little difference in the Mulliken partial charges of the atoms in the molecules. Only the C atom bonded to the Zn atom has a slightly more negative value of −0.3 vs. −0.1 in the Mes and Ph groups, respectively. Consequently, the Zn–C bond is slightly shorter in **6**. It is not possible to draw any significant conclusions from the differences between **1** and **6** with regards to the overall reaction cascade and the influence of the ligand sphere of the starting material, though there are slight differences on the geometric parameters of the two structures.

Calculations of the reaction energies for the formation of anions **1**, **2**, and **6** (Scheme S1) in a first step according to equation (1) confirmed the expected trend. The reactivity of the complex fragment with R being C_6F_5 causes the most exoenergetic reaction (−438 kJ mol^{-1}), followed by the one with R = Ph (−392 kJ mol^{-1}) and finally the one with R = Mes (−387 kJ mol^{-1}).

$$(Ge_3As)^3 + [ZnR]^+ \rightarrow [RM(Ge_3As)]^2 \quad (1)$$

We note in passing that the formation of this anion type is energetically preferred over a hypothetical '$[RM(Ge_2As_2)]^-$' comprising a $(Ge_2As_2)^{2-}$ group (e.g., reaction energy for R/M = Ph/Zn −359 kJ mol^{-1}; Scheme S1). In accordance with the numbers shown in Figure 2, it is advantageous to avoid an As atom at the apex opposite the organic group, which is unlikely if $(Ge_2As_2)^{2-}$ is the coordinating species.

Regarding the second step to form anion **3** (Equation (2) and Scheme S2), the release and replacement of the C_6F_5 substituent is (again) the most exoenergetic (−256 kJ mol^{-1}), followed by the process involving Ph (−251 kJ mol^{-1}) and then the one involving Mes (−238 kJ mol^{-1}). This may (in part) be ascribed to the fact that equation (2) formulates the recovery of $[ZnR_2]$, but also other possible fates of the substituents (like formation of RH upon deprotonation the solvent en) show the same trend.

$$[RZn(Ge_3As)]^2 + (Ge_2As_2)^2 + [ZnR]^+ \rightarrow [(Ge_3As)Zn(Ge_2As_2)]^3 + [ZnR_2] \quad (2)$$

Although the differences are not very large, the trend is in line with the experimental observation of a rather quick release of C_6F_5 (similar to Cl^- from $ZnCl_2$) from the reactant(s) and degradation of the reaction mixture, and also congruent with the tendency of the Ph compound to smoothly continue cluster growth, while the Mes compound reacts less readily.

For comparison, we also studied reactions towards hypothetical alternatives, '$[(Ge_2As_2)Zn(Ge_2As_2)]^{2-}$' or '-$[(Ge_3As)Zn(Ge_3As)]^{4-}$', from a hypothetical anion '$[PhZn(Ge_2As_2)]^-$' or the anion **1**, respectively (Scheme S2). Interestingly, both would be energetically favorable, so they could form but do not crystallize owing to a mismatch of the cluster charge and size with the required number of [K(crypt-222)]$^+$ counterions, in contrast to a good match in case of anion **3** (see next section).

In [K(crypt-222)]$_3$(**3**), the Zn atom is coordinated by two different *pseudo*-tetrahedral anions, one $(Ge_2As_2)^{2-}$ and one $(Ge_3As)^{3-}$ (Figure 3). We derive this from *pseudo*-element considerations again: for a total of three negative charges, the Zn^{2+} ion must be combined with anionic 'ligands' of 5 charges altogether, which is congruent with the named composition. Both 'ligands' are coordinated through the atoms of a Ge–Ge edge (η^2-coordination mode), producing an overall distorted tetrahedral geometry around the Zn atom. However, the most interesting aspect of the anion **3** is the occurrence of two different ligands. While it was reported that the same type of ligands can coordinate in different fashions to the same metal center in such assemblies, the occurrence of two differently charged *pseudo*-tetrahedra has not yet been realized. Assuming that the $(ZnPh)^+$ unit could initially interact with both of them, hence leading to anion **1** or a yet unidentified alternative with the formula '$[PhZn(Ge_2As_2)]^-$', the next step is the replacement of the second phenyl substituent with the other binary anion.

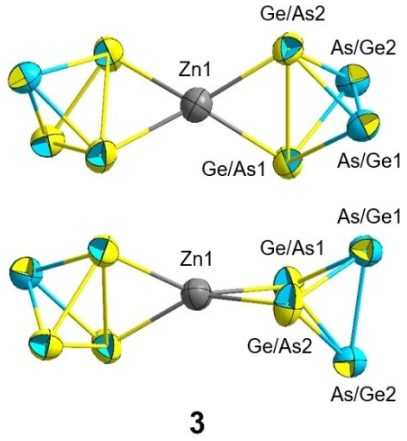

Figure 3. Two different views of the molecular structure of the anion $[(Ge_2As_2)Zn(Ge_3As)]^{3-}$ (**3**) in compound [K(crypt-222)]$_3$(**3**), with thermal ellipsoids drawn at 50% probability. Since Ge and As atoms cannot be distinguished, the corresponding atom types are drawn in two-colored fashion (yellow-blue), with the more probable atom according to quantum chemical calculations being indicated by the dominant color (see text). Selected distances [Å] and angles [°]: Zn Ge/As 2.5239(9)–2.5240(9), Ge/As1 Ge/As2 2.7360(10), As/Ge1 As/Ge2 2.4968(10), Ge/As As/Ge 2.4594(12)–2.4771(10); Zn Ge/As Ge/As 56.97(3), 100.75(4)–108.38(4), angles within the Ge/As *pseudo*-tetrahedra 56.04(3)–67.31(3).

Considering the successful isolation of **1** led to the speculation that in the reaction that affords **3**, we first see the formation of **1** before the Ph group is then substituted by a $(Ge_2As_2)^{2-}$ anion in a second step. As mentioned above, calculation of the reaction energy shows this second step to also be strongly exoenergetic (Scheme S2). According to the experience in Zintl cluster chemistry, the main reason for anion **1** to form an isolable salt instead of the mentioned alternative, and the reason for **3** to crystallize along with $[K(crypt\text{-}222)]^+$ cations, while the other possible variants with either two $(Ge_2As_2)^{2-}$ 'ligands' (**A**; two negative charges in total) or two $(Ge_3As)^{3-}$ 'ligands' (**B**; four negative charges in total) do not, is simply a matter of the resulting lattice energy. Obviously, the combination of one cluster anion of charge 3– with three $[K(crypt\text{-}222)]^+$ cations produces the lowest solubility under the given conditions (higher charges require K^+ counterions in neat solids, see above). We cannot see a reason why the other species should generally not form (and mass spectra do give hints for other than the crystallized anions to exist), but in the absence of crystallographic data for them, this is mere speculation. However, the observation of potential follow-up products of variant **B** seem to underscore these thoughts, as discussed in the following.

It should be noted that the computational optimization of the geometry of the anion in **3** without symmetry restrictions did not yield the structure depicted in Figure 3. Instead, the $(Ge_3As)^{3-}$ 'ligand' coordinates the Zn atom the same way as in **1**, hence in an η^3-fashion. Fixation of the respective dihedral angles during the optimization, however, yielded the structure as found in **3** (see Figure S96). The difference between the absolute energies of the global minimum and the local minimum under symmetry restrictions is not significant in context of the chosen DFT methods (5 kJ mol^{-1}), which is plausible, considering the only weak interaction between the As and the Zn atom in **1**. We thus attribute the observation of the structure as shown in Figure 3 to the energy differences in the lattice energy caused by the assumed different packing modes of cations and the different isomeric anions in the crystal structure.

Anion **4** represents the heavier congener of the previously reported $[Cd_3(Ge_3P)_3]^{3-}$ cluster anion, and also shows the same pinwheel-like structure (Figure 4). The elemental composition was determined with the help of both the total charge/*pseudo*-element considerations and from energy-dispersive X-ray spectroscopy (EDS). As corroborated by quantum chemistry, the assignment of As and Ge atoms is the same as for the lighter congener, all three *pseudo*-tetrahedra act as η^2:η^3-μ-bridging ligands, thereby using exclusively the Ge atoms for coordination. This

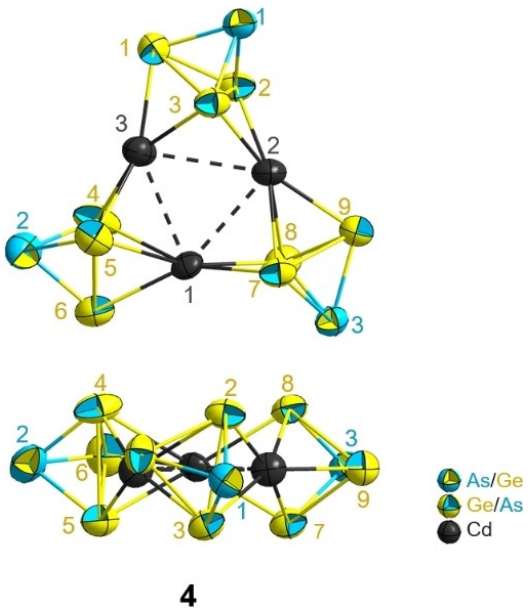

Figure 4. Top view (top) and side view (bottom) of the oblate molecular structure of the anion $[Cd_3(Ge_3As)_3]^{3-}$ (**4**) in compound $[K(crypt\text{-}222)]_3$(**4**)·tol, with thermal ellipsoids drawn at 50% probability. Since Ge and As atoms cannot be distinguished, the corresponding atom types are drawn in two-colored fashion (yellow-blue), with the more probable atom according to quantum chemical calculations being indicated by the dominant color; in addition, a corresponding color code was used for the atom labels (see bottom right). Selected distances [Å] and angles [°]: Cd...Cd: 3.23(3)–3.403(9), Cd Ge/As: 2.697(12)–3.02(3), Ge/As As/Ge: 2.385(11)–2.459(11), Ge/As Ge/As: 2.552(13)–2.890(11); Ge/As Cd Ge/As 53.1(6)–63.5(2), 113.9(3)–165.0(3), Cd...Cd Ge/As 52.0(2)–62.8(2)., 91.3(3)–111.1(6), 148.4(5)–157.2(11), Cd Ge/As Ge/As 57.3(2)–76.2(4), 106.3(4)–112.9(3), Cd Ge/As As/Ge 98.5(6)–111.6(5), Cd Ge/As Cd 68.0(6)–75.8(3), angles within the Ge/As *pseudo*-tetrahedra 52.2(3)–74.2(3).

observation is not only congruent with the formal assignment of negative charges to these atoms (which in fact is pretty much smeared over the whole *pseudo*-tetrahedron for the isolated species), but also with the nature of the HOMO of all of these binary analogues of white phosphorous: the HOM O always comprises main contributions from Ge atoms, which are therefore the most Lewis-basic sites of the anions. A population analysis based on occupation numbers and the calculation of shared electron numbers confirmed the absence of significant Cd···Cd interactions (see Table S26).

The cluster **4** indicates that the Cd analogue of a hypothetical **3'** variant of anion **3** may have formed in solution, which could not crystallize along with $[K(crypt\text{-}222)]^+$ cations unless being complemented by two more M^{2+} anions and another $(Ge_3As)^{3-}$ unit. Although the Cd homologue of compound **3** has not yet been isolated, a similar start of the reaction cascade appears to be very plausible; ESI mass spectra of a fresh solution of single crystals of the compound comprising anion **4** show the signal of a corresponding fragment $(CdGe_5As_3C_7H_{10})^-$ (see Figure S65), which is not a proof of the formation of **4** from this species but indicates a chemical relationship. Furthermore, as mentioned at the outset, we are confident that we also synthesized the corresponding Zn homologue of **4**, '$[Zn_3(Ge_3As)_3]^{3-}$', as suggested from preliminary X-ray diffraction data and ESI-MS analyses of the reaction solution yielding compounds (see Figures S44, S45, S48, and S50). Again, three charges seem to fulfil the minimum precondition for crystallization of this anion with the available cations, although a lower crystal quality as compared to the compounds comprising anions **1**–**3** already indicates a deviation from an ideal fit.

Similarly as discussed above for the different substituents, comparison of the reaction energies involving Zn and Cd atoms helps to understand the direct formation of **4** for M = Cd, while M = Zn allows for an observation of intermediate steps: for R being Ph, reaction energies are $-392\ kJ\,mol^{-1}$ and $-251\ kJ\,mol^{-1}$ (Zn) or $-462\ kJ\,mol^{-1}$ and $-334\ kJ\,mol^{-1}$ (Cd) for the first and second step, respectively, indicating a preference for continuous cluster growth with the heavier metal. The reaction energies obtained for M = Hg ($-490\ kJ\,mol^{-1}$ and $-378\ kJ\,mol^{-1}$) would suggest an even higher reaction tendency toward cluster growth, in this regard, the crystallization of **2** (and not a compound similar to **3** or **4**) is somewhat surprising and lucky. The fact that the larger clusters are not obtained with M = Hg can be explained by the overall much higher sensitivity of the reaction solution that decomposes much more quickly than those of the Zn and Cd reactants.

An alternative to the pinwheel structure obviously forms if two Zn^{2+} and two $(Ge_3As)^{3-}$ anions are added to the **3'**-type variant of compound **3**: in $[K(crypt\text{-}222)]_9$(**5a**)-(**5b**)$_{0.5}$·en, three Zn^{2+} and a total of four $(Ge_3As)^{3-}$ 'ligands' form a chain-like coordination oligomer $[(Ge_3As)Zn(Ge_3As)Zn(Ge_3As)Zn(Ge_3As)]^{6-}$ (**5**; Figure 5), which nicely demonstrates the continuation of the coordination of *pseudo*-tetrahedral anions to group 12 metal ions. Two of the *pseudo*-tetrahedra act as η^2:η^2-μ-type bridges, and two terminal units represent η^2-ligands.

Apparently, the oligomer growth was terminated at this stage with a total anionic charge of 6−. For the given size, any lower charge which could have been realized upon inclusion of $(Ge_2As_2)^{2-}$ units instead of $(Ge_3As)^{3-}$ seems to be more unfavorable. An anion of a similar topology but higher charge was reported to exist in the ternary solid K_6CdPb_8, $[Pb_4CdPb_4CdPb_4CdPb_4]^{10-}$ (besides Pb_4^{4-} anions).[5a] Here, the Pb_4^{4-} ligands act as η^3:η^3-μ ligands or η^3-ligands, which results in near octahedral coordination of the Cd^{2+} cations and a zig-zag-type shape of the oligomer—hence markedly different from the anion **5**.

The crystal structure comprises two conformers of the anion in a 1:0.5 ratio, **5a** and **5b**, which apart from statistical disorder and structural details are very similar regarding the overall connection of Zn^{2+} ions and *pseudo*-tetrahedral units (Figure 5). In **5a**, all atoms are placed on general positions. However, anion **5b** is located on an inversion center, thus producing a second set of split positions which requires all atoms to be refined as partly occupied (50% in most cases; for more details, see Figure S15). Owing to the role of the *pseudo*-tetrahedra acting as either μ-η^2:η^2 bridges or η^2-type terminal ligands, the coordination environments of all Zn^{2+}

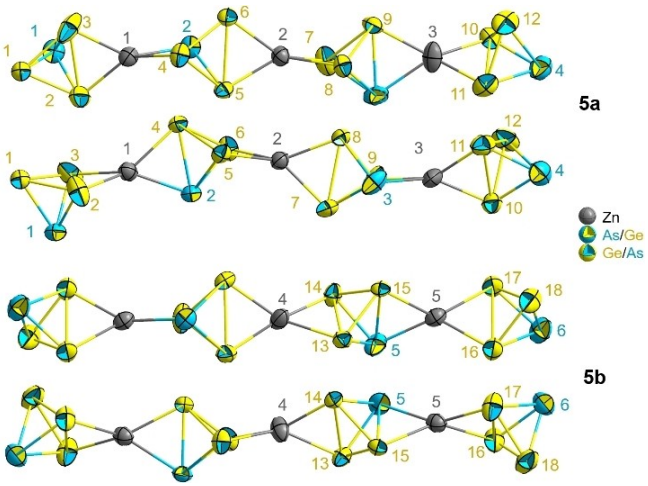

Figure 5. Two different views each of the molecular structures of the two crystallographically independent $[Zn_3(Ge_3As)_4]^{6-}$ anions in compound $[K(crypt\text{-}222)]_9(\mathbf{5a})(\mathbf{5b})_{0.5}\cdot en$, **5a** (top) and **5b** (bottom), with thermal ellipsoids drawn at 50% probability. Since Ge and As atoms cannot be distinguished, the corresponding atom types are drawn in two-colored fashion (yellow-blue), with the more probable atom according to quantum chemical calculations being indicated by the dominant color; in addition, a corresponding color code was used for the atom labels (see center right). Note that within **5a**, Ge/As1, is isotropic. Selected distances [Å] and angles [°]: Zn Ge/As 2.332(10)–2.658(7), Zn As/Ge 2.535(2)–2.589(3), Ge/As Ge/As 2.416(6)–2.769(2), Ge/As As/Ge 2.431(3)–2.6752(19); angles within the *pseudo*-tetrahedra 55.29(6)–68.94(11).

ions represent (elongated) tetrahedra, as is typical for four-coordinate Zn^{2+} ions.

While the elemental composition of the anions **5** is plausible based on the *pseudo*-element concept, as was confirmed by means of μ-XFS analyses, the assignment of Ge and As atoms along the chain-type anions remained an open question. We anticipated that the terminal *pseudo*-tetrahedra would again prefer Ge atoms for coordination, but the μ-bridging ones were forced to use all four atoms for coordination with no predictable preference for the position of the single As atom per *pseudo*-tetrahedron. We note that based on the relatively regular interatomic distances, we ruled out a coexistence of three different types of binary anions (with three different charges), which would have been necessary if distributing the Ge and As atoms over the whole cluster in a different way than by assignment of a Ge : As ratio of 3 : 1 for all of the binary units.

For the most probable assignment of Ge and As atoms, quantum chemistry was employed once more. The DFT calculations converged into a structure exhibiting a distorted tetrahedral coordination environment around the central Zn atom. Assigning the As atoms on different positions in each *pseudo*-tetrahedral moiety lead to six conformers within $\approx 20\ kJ{\cdot}mol^{-1}$ of relative energy. Additionally, the absolute energy of a hypothetical conformer with a planar coordination sphere around the central Zn atom was found to be $18\ kJ{\cdot}mol^{-1}$ higher than for the global minimum structure (Figure S99). In the presumed global minimum structure, we find the central Zn atom solely coordinated by Ge atoms and the two outer Zn atoms by no more than one As atom of the two inner $(Ge_3As)^{3-}$ moieties. The bond lengths and angles are within the expected range (see Tables S10 and S11).

As discussed within this report, we hypothesize that the anions in compounds **1**–**5** are, not only structurally, but also chemically related, and represent snapshots along a formation cascade. This, however, is not a straight line, but rather follows different 'evolutionary branches' of cluster formation. The fact that the extraction solution of 'K_2GeAs' provides us with (at least) two different binary *pseudo*-tetrahedral anions allows us to track these branches, while homoatomic anions would lead to other products with different charges. Scheme 2 summarizes the findings in this work, thereby including previous findings with Ge_4^{4-} anions for completeness. Note that the Scheme was drawn based on experimental observations (with R = Ph), as theoretical pathway studies that include small clusters of different (anionic) charges do not produce reliable reaction profiles. The computations of reaction energies discussed above, however, provided a rationale for the first steps to be feasible in the way shown here.

Besides the obvious development of the aggregation pathway shown in Scheme 2, we also include the 'intermediate' species comprising two $(Ge_3As)^{3-}$ anions and one M^{2+} cation (**3'**, see above); as it has not (yet) been observed, it is drawn in grey shade. For a most straight-forward pathway, we consider its occurrence during the formation of the larger aggregates plausible. However, we do not expect to crystallize this anion owing to its high charge. Of course, we cannot rule out more complicated multi-step exchange reactions to take place involving species with $(Ge_2As_2)^{2-}$ (and $(Ge_3As)^{3-}$) anions as ligands, such as the one given on the left hand side of Scheme 2, but it would be much more difficult to argue for it.

Formally, the equilibrium shown in the top row could proceed towards the homoatomic tetrahedra, and ESI-MS gives hints for the occurrence of $\{Ge_4\}$ units, but no products have been isolated in crystalline form from such solutions comprising homoatomic Ge_4^{4-} anions. This part of the equilibrium is therefore given in grey characters, too, and

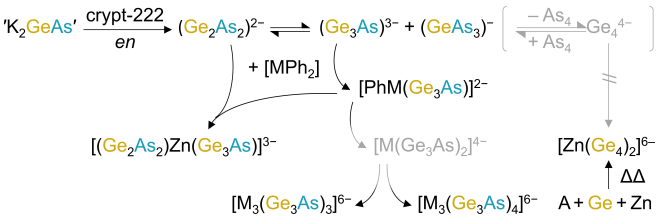

Scheme 2. Suggestion for the reaction branches that may occur for the combination of an extraction solution of 'K_2GeAs' in en/crypt-222 with $[MPh_2]$, to afford cluster anions such as reported in this work (center and left) based on single-crystal X-ray diffraction or mass spectrometry studies. Formulas given in grey shade refer to hypothetical species that have not (yet) been detected. Arrows with a black/grey color gradient indicate unproven, yet plausible steps towards and from such species, while unsubstantiated paths are crossed out for clarity. M = Zn, Cd, and/or Hg; A = K, Rb, or Cs.

the corresponding pathway towards related clusters comprising Ge_4^{4-} anions is crossed out. Such clusters were obtained by solid state reactions of the elements instead (right), hence in the Zintl phases $A_{14}ZnGe_{16}$ (A = K, Rb)[7c] or Cs_6Ge_8Zn,[4] as the very high charge density requires the close proximity of alkali metal ions—and not the bulky $[A(cypt\text{-}222)]^+$ complexes with their comparably low charge density. Noteworthy however, a related complex with a protonated $\{Ge_4\}$ unit, $[\{\eta^2\text{-}(HGe_4)\}ZnPh_2]^{3-}$, was obtained from the reaction of the extraction solution of $K_6Rb_6Ge_{17}$ in en/crypt-222 with $[ZnPh_2]$.[18] This indicates some flexibility of the reaction space including homoatomic units, too, by protonation.

Conclusion

In conclusion, we were able to isolate a series of anionic clusters comprising one, two, three, or four *pseudo*-tetrahedral p-block element units $(Ge_{3-x}As_{1+x})^{(3-x)-}$ ($x = 0$, 1) by reacting an extraction solution of the solid 'K_2GeAs' in en/crypt-222 with $[MPh_2]$ (M = Zn, Cd, Hg). The anions within the crystalline products, $[PhZn(Ge_3As)]^{2-}$ (**1**), $[PhHg(Ge_3As)]^{2-}$ (**2**), $[(Ge_3As)Zn(Ge_2As_2)]^{3-}$ (**3**), $[Cd_3(Ge_3As)_3]^{3-}$ (**4**), $[Zn_3(Ge_3As)_4]^{6-}$ (**5**), and $[MesZn(Ge_3As)]^{2-}$ (**6**) demonstrate that the extraction of 'K_2GeAs' indeed affords different As_4-analogous species, $(Ge_2As_2)^{2-}$ and $(Ge_3As)^{3-}$, which seem to co-exist in an equilibrium. Mass spectra indicate also $(GeAs_3)^-$ to be present. The two former *pseudo*-tetrahedra were picked by M^{2+} cations or $[MPh]^+$ fragments to form clusters with various architectures, varying from the attachment of a $(PhM)^+$ unit to one $(Ge_3As)^{3-}$ anion to a chain-type structure comprising four of them beside three M^{2+}.

Our comprehensive study combining X-ray diffraction analyses, mass-spectrometry, and quantum chemical calculations shows that 1) there are notable differences in the reactivity and stability of the Zn-, Cd-, or Hg-based reactants and products, but 2) that we can generally find many analogous species in all sets of reactions. The different reactivities/stabilities (and possibly also solubilities) do not allow for the crystallization of them all though.

The products of the reactions discussed herein do not only provide insight into the Ge/As/(Ph)M reaction space and enrich the structural variety of compounds forming therein, but also help to understand stepwise cluster formation under selection of the most suitable binary species from the ones offered in situ. In future investigations, we will use organometallic compounds of other d-/f-block metals to explore their influence on cluster formation and product spectra obtained from the K/Ge/As Zintl system.

Acknowledgements

This work was supported by the German Research Foundation (Deutsche Forschungsgemeinschaft, DFG). L.G. thanks Dr. Uwe Huniar of Dassault Systèmes Deutschland GmbH and Prof. Dr. F. Weigend for valuable help with TmoleX. We are grateful to Dr. S. Ivlev for his help with X-ray diffraction studies and refinements. Open Access funding enabled and organized by Projekt DEAL.

Conflict of Interest

The authors declare no conflict of interest.

Data Availability Statement

The data that support the findings of this study are available in the supplementary material of this article.

Keywords: As_4 Analogues · DFT Calculations · Group 12 Metals · X-Ray Diffraction · Zintl Anions

[1] D. E. C. Corbridge, *Phosphorus 2000: chemistry, biochemistry & technology*, Elsevier, Amsterdam, **2000**.

[2] a) M. Scheer, G. Balázs, A. Seitz, *Chem. Rev.* **2010**, *110*, 4236–4256; b) T. Li, S. Kaercher, P. W. Roesky, *Chem. Soc. Rev.* **2014**, *43*, 42–57; c) P. Dapporto, S. Midollini, L. Sacconi, *Angew. Chem. Int. Ed. Engl.* **1979**, *18*, 469–469; d) F. Spitzer, M. Sierka, M. Latronico, P. Mastrorilli, A. V. Virovets, M. Scheer, *Angew. Chem. Int. Ed.* **2015**, *54*, 4392–4396.

[3] a) R. Schäfer, W. Klemm, *Z. Anorg. Allg. Chem.* **1961**, *312*, 214–220; b) E. Busmann, *Z. Anorg. Allg. Chem.* **1961**, *313*, 90–106; c) U. Zachwieja, J. Müller, J. Wlodarski, *Z. Anorg. Allg. Chem.* **1998**, *624*, 853–858; d) Y. Morino, T. Ukaji, T. Ito, *Bull. Chem. Soc. Jpn.* **1966**, *39*, 64–71; e) A. Bettendorff, *Ann. Chem. Pharm.* **1867**, *144*, 110–114; f) M. Cossairt Brandi, M. C. Diawara, C. C. Cummins, *Science* **2009**, *323*, 602; g) S. Mitzinger, J. Bandemehr, K. Reiter, S. J. McIndoe, X. Xie, F. Weigend, J. F. Corrigan, S. Dehnen, *Chem. Commun.* **2018**, *54*, 1421–1424; h) S. Mitzinger, L. Broeckaert, W. Massa, F. Weigend, S. Dehnen, *Nat. Commun.* **2016**, *7*, 10480–10490; i) F. Lips, I. Schellenberg, R. Pöttgen, S. Dehnen, *Chem. Eur. J.* **2009**, *15*, 12968–12973; j) S. C. Critchlow, J. D. Corbett, *Inorg. Chem.* **1982**, *21*, 3286–3290; k) F. Lips, M. Raupach, W. Massa, S. Dehnen, *Z. Anorg. Allg. Chem.* **2011**, *637*, 859–863; l) R. Ababei, J. Heine, M. Hołyńska, G. Thiele, B. Weinert, X. Xie, F. Weigend, S. Dehnen, *Chem. Commun.* **2012**, *48*, 11295–11297; m) L. Xu, S. C. Sevov, *Inorg. Chem.* **2000**, *39*, 5383–5389; n) N. Lichtenberger, N. Spang, A. Eichhöfer, S. Dehnen, *Angew. Chem. Int. Ed.* **2017**, *56*, 13253–13258; o) L. Guggolz, S. Dehnen, *Chem. Eur. J.* **2020**, *26*, 11819–11828.

[4] V. Queneau, S. C. Sevov, *J. Am. Chem. Soc.* **1997**, *119*, 8109–8110.

[5] a) E. Todorov, S. C. Sevov, *Angew. Chem. Int. Ed.* **1999**, *38*, 1775–1777; b) D. Huang, J. D. Corbett, *Inorg. Chem.* **1998**, *37*, 5007–5010.

[6] a) J. D. Corbett, D. G. Adolphson, D. J. Merryman, P. A. Edwards, F. J. Armatis, *J. Am. Chem. Soc.* **1975**, *97*, 6267–6268; b) T. F. Fässler, R. Hoffmann, *Angew. Chem. Int. Ed.* **1999**, *38*, 543–546.

[7] a) M. Waibel, F. Kraus, S. Scharfe, B. Wahl, T. F. Fässler, *Angew. Chem. Int. Ed.* **2010**, *49*, 6611–6615; b) M. Waibel, G. Raudaschl-Sieber, T. F. Fässler, *Chem. Eur. J.* **2011**, *17*, 13391–13394; c) S. Stegmaier, M. Waibel, A. Henze, L. A. Jantke, A. J. Karttunen, T. F. Fässler, *J. Am. Chem. Soc.* **2012**, *134*, 14450–14460.

[8] a) M. Waibel, T. Henneberger, L. A. Jantke, T. F. Fässler, *Chem. Commun.* **2012**, *48*, 8676–8678.

[9] C. B. Benda, M. Waibel, T. Köchner, T. F. Fässler, *Chem. Eur. J.* **2014**, *20*, 16738–16746.
[10] F. Fendt, C. Koch, S. Gärtner, N. Korber, *Dalton Trans.* **2013**, *42*, 15548–15550.
[11] H. L. Xu, I. A. Popov, N. V. Tkachenko, Z. C. Wang, A. Muñoz-Castro, A. I. Boldyrev, Z. M. Sun, *Angew. Chem. Int. Ed.* **2020**, *59*, 17286–17290.
[12] F. Pan, L. Guggolz, S. Dehnen, *CCS Chem.* **2022**, *4*, 809–824.
[13] F. Pan, L. Guggolz, F. Weigend, S. Dehnen, *Angew. Chem. Int. Ed.* **2020**, *59*, 16638–16643.
[14] a) R. J. Wilson, N. Lichtenberger, B. Weinert, S. Dehnen, *Chem. Rev.* **2019**, *119*, 8506–8554; b) F. Pan, L. Guggolz, S. Dehnen, *Nat. Sci.* **2022**, *2*, e202103302; c) R. J. Wilson, L. Broeckaert, F. Spitzer, F. Weigend, S. Dehnen, *Angew. Chem. Int. Ed.* **2016**, *55*, 11775–11780.
[15] J. M. Goicoechea, S. C. Sevov, *Organometallics* **2006**, *25*, 4530–4536.
[16] Deposition numbers 2195385 ($[K(crypt\text{-}222)]_2(\mathbf{1})_{0.9}\cdot(Ge_2As_2)_{0.1}\cdot 0.9tol$), 2195386 ($[K(crypt\text{-}222)]_2(\mathbf{2})\cdot tol$), 2195387 ($[K(crypt\text{-}222)]_3(\mathbf{3})$), 2195388 ($[K(crypt\text{-}222)]_3(\mathbf{4})\cdot tol$), 2195389 ($[K(crypt\text{-}222)]_9(\mathbf{5a})(\mathbf{5b})_{0.5}\cdot en$), and 2233616 ($[K(crypt\text{-}222)]_2(\mathbf{6})$) contain the supplementary crystallographic data for this paper. These data are provided free of charge by the joint Cambridge Crystallographic Data Centre and Fachinformationszentrum Karlsruhe Access Structures service.
[17] a) TURBOMOLE V7.5.1 **2021**, a development of University of Karlsruhe and Forschungszentrum Karlsruhe GmbH, 1989–2007, TURBOMOLE GmbH, since 2007; available from http://www.turbomole.com; b) TmoleX: C. Steffen, K. Thomas, U. Huniar, A. Hellweg, O. Rubner, A. Schroer, *J. Comput. Chem.* **2010**, *31*, 2967–2970.
[18] C. Wallach, K. Mayer, T. Henneberger, W. Klein, T. F. Fässler, *Dalton Trans.* **2020**, *49*, 6191–6198.